

# Therapeutic Effect of Calcipotriol Pickering Nanoemulsions Prepared by Exopolysaccharides Produced by *Bacillus halotolerans* FYS Strain on Psoriasis

This article was published in the following Dove Press journal:  
*International Journal of Nanomedicine*

Yuzhen Wang<sup>1</sup>  
Hong Li<sup>2</sup>  
Fakun Dong<sup>3</sup>  
Fang Yan<sup>3</sup>  
Min Cheng<sup>4</sup>  
Wanzhong Li<sup>3</sup>  
Qi Chang<sup>3</sup>  
Tianzi Song<sup>3</sup>  
Aoying Liu<sup>3</sup>  
Bo Song<sup>3</sup>

<sup>1</sup>Medical Imaging Specialty, Weifang Medical University, Weifang, Shandong, People's Republic of China; <sup>2</sup>Basic Medical School, Weifang Medical University, Weifang, Shandong, People's Republic of China; <sup>3</sup>School of Pharmacy, Weifang Medical University, Weifang, Shandong, People's Republic of China; <sup>4</sup>Clinical Medical College, Weifang Medical University, Weifang, Shandong, People's Republic of China

**Purpose:** Many exopolysaccharides (EPS) have significant emulsifying activity. Some EPS produced by the marine bacterial strain FYS have stronger emulsifying activity in the form of nanoparticles, suggesting that they could potentially form Pickering emulsions. We prepared novel EPS/CT Pickering nanoemulsions (ECPN) with EPS as emulsifiers and assessed their ability to ameliorate the poor permeability of calcipotriol (CT) in skin affected by psoriasis vulgaris.

**Methods:** A strain of marine bacterium FYS was identified. Molecular weight, monosaccharide composition and microstructure of EPS were determined by gel permeation chromatography, high-performance liquid chromatography and scanning electron microscopy. EPS nanoparticles were prepared by adjusting the pH, and the emulsifying activity was studied at different pH. ECPN were prepared by ultrasound and optimized by the response surface method. The size distribution, microstructure, stability and in vitro drug release of ECPN were studied. The therapeutic effect of ECPN on psoriasis vulgaris was explored by animal experiments and characterizing histomorphology in vivo.

**Results:** A phylogenetic tree revealed that FYS was a *Bacillus halodurans* strain. EPS produced by the strain were heteropolysaccharides with a three-dimensional network composed of glucose, galactose, glucuronic acid, rhamnose, galacturonic acid and mannose (32.0:34.3:9.7:7.4:10.3:6.3). The EPS can form nanoparticles at pH = 4–6 with enhanced emulsifying ability. Transmission electron microscopy revealed that EPS nanoparticles adhered to the surface of oil droplets to stabilize the emulsions via a Pickering emulsification mechanism. The prepared ECPN have high stability with a sustained-release effect. Finally, animal experiments showed that ECPN effectively shortened the treatment course of psoriasis vulgaris.

**Conclusion:** EPS is highly possible to have the potential Pickering emulsification mechanism. The stability of the nanoemulsion was high. ECPN also showed potential for use in the treatment of psoriasis vulgaris. This study provides new insight into the medical applications of EPS and the treatment of psoriasis.

**Keywords:** *Bacillus halotolerans*, exopolysaccharides, response surface method, psoriasis

## Introduction

Exopolysaccharides (EPS) are long-chain polymers secreted by microorganisms that have been widely used as emulsifiers, thickeners or gelling agents in medicine, food and industry.<sup>1</sup> Emulsifying activity is one of the most important properties of EPS.<sup>2</sup> EPS can form an expanded network or a layer of emulsion film in

Correspondence: Bo Song  
Weifang Medical University, Baotong  
Street, No. 7166, Weifang, Shandong  
261053, People's Republic of China  
Tel/Fax +86-536-8462490  
Email songsbob@163.com

a continuous phase to stabilize emulsions. Compared with emulsifiers from chemical sources (such as Span 80 and Tween 80), the efficacy of EPS can be achieved at lower application rates (mostly 1.0–2.0%); furthermore, EPS is characterized by strong emulsifying ability, low toxicity and good biocompatibility, suggesting that they have great potential to be used as emulsifiers.<sup>3</sup>

Psoriasis is a major skin disease worldwide, and most efforts to treat it have employed local symptomatic treatment.<sup>4</sup> Commonly used drugs include keratolytics, glucocorticoids, retinoic acids, vitamin D3, calcium-phosphorus nerve phosphatase inhibitors and tar.<sup>5</sup> Systemic medication therapies are less safe. For example, methotrexate injection may cause irreparable damage to pregnant women and fetuses.<sup>6</sup> Therefore, long-term use of topical drugs is still a common means of treatment.<sup>7</sup> Calcipotriol (CT) is a first-line drug for the topical treatment of psoriasis vulgaris that can correct the abnormal proliferation and differentiation of keratinocytes (KCs), regulate the inflammatory response and reduce the number of T cells in psoriatic lesions.<sup>8</sup> CT is mainly applied in topical dosage forms, such as cream (0.005%) and liniment (0.005%). Rough psoriatic skin is a major barrier to the percutaneous penetration of topical drugs because of the formation of scaly plaques and thickening of the epidermis. Thus, developing ways by which drugs can effectively penetrate the epidermis remains a major challenge.

Nanoemulsions (NE) are liquid systems tens to hundreds of nanometers in size that are composed of water, emulsifier (co-emulsifier) and oil in appropriate proportions. NE have low surface tension and can easily wet the skin or affect skin structure to promote drug penetration when administered transdermally. They also have the advantages of promoting drug absorption in target tissues, prolonging action time and requiring lower application rates to achieve efficacy, properties that are especially suitable for skin diseases.<sup>9</sup> With the development of nanotechnology, the research on EPS in NE has gradually emerged. For example, EPS produced by *Bacillus vallis-mortis* WF4 strain can form an emulsifying film on the surface of droplets to stabilize NE.<sup>10</sup> In recent years, Pickering emulsification has become a major subject of research, especially the ability of solid particles to replace surfactants as emulsifiers to form Pickering emulsions or NE.<sup>11</sup> The solid particles irreversibly adsorb on the oil-water interface, forming a stable three-dimensional network structure in the continuous phase to prevent the collision and coalescence between droplets.<sup>12</sup> In addition,

Pickering NE have attracted much attention for its advantages, including its low toxicity, environmentally friendly properties, low emulsifier consumption and easy preparation.<sup>13</sup> Previous studies have shown that many inorganic nanoparticles, such as SiO<sub>2</sub> nanoparticles,<sup>14</sup> Fe<sub>3</sub>O<sub>4</sub> nanoparticles and clay particles,<sup>15</sup> are capable of forming Pickering NE. However, these particles have poor degradability, limiting their applications. Thus, much effort has been made to seek new and safe Pickering emulsifiers with higher emulsifying activity.<sup>15</sup> However, EPS in Pickering emulsification have not been studied to date.

Here, we prepared a new and stable EPS/CT Pickering NE (ECPN) using pH-sensitive EPS produced by the marine mangrove bacterium *Bacillus halotolerans* as an Pickering emulsifier, with the goal of enhancing the penetration of common CT dosage forms into psoriatic skin. Finally, the therapeutic effect of ECPN on psoriasis vulgaris was studied using an animal experiment. We confirmed the Pickering emulsification capability of EPS for the first time. Generally, our findings help promote in-depth applications of EPS as a medical material as well as new ideas for improving the therapeutic efficacy of treatments for psoriasis vulgaris.

## Materials and Methods

### Materials and Reagents

A strain producing EPS (FYS strain) was screened from the marine mangrove system, using peptone 10.0 g/L, yeast 10.0 g/L and glucose 5.0 g/L (pH=6.5–7.0) as the fermentation medium. Sunflower oil was purchased from Shandong Luhua Group Co., Ltd., China. CT was obtained from Shanghai Macklin<sup>®</sup> Reagent Co., Ltd. (Shanghai, China). Daivonex (CT scalp solution) was obtained from LEO Pharma A/S (Ballerup, Copenhagen, Denmark). Imiquimod cream was purchased from Sichuan Mingxin Pharmaceutical Co., Ltd. (Chengdu, China). Mice were provided by the Experimental Animal Center of Weifang Medical College.

### Strain Identification

Routine identification of the FYS strain was performed following the methods of Sambrook (1989).<sup>16</sup> The 16S rDNA genome of the FYS strain was simultaneously amplified using two primers (forward primer: 5'-CAGAGTTTGATCCTGGCT-3'; reverse primer: 5'-AGGAGGTGATCCAGCCGCA-3'). Sequencing results

were compared (<http://www.ncbi.nlm.nih.gov/BLAST>), followed by comparison using Clustal X1.81 software; phylogenetic trees were constructed using MEGA 5.0.<sup>17</sup>

## Fermentation and Preparation of EPS

After inoculation with 100.0 mL of liquid medium, the seed liquid was cultured after 10 h of shaking at 37°C and 180 rpm, followed by culture in 2 L of liquid medium ( $OD_{600\text{ nm}} = 0.6\text{--}0.8$ ) at a ratio of 2.0% and fermentation at 37°C and 180 rpm for 40 h. The above fermentation broth was centrifuged at 10,000 g for 5 min, and the supernatant was filtered with a microporous filter membrane (0.45  $\mu\text{m}$ ), concentrated by rotary evaporation and cooled to 4°C in a refrigerator. The pH of the concentrated solution was adjusted to 1.0–2.0 with concentrated HCl at a ratio of 4.0%. The solution was cooled overnight at 4°C until precipitation of a large amount of white flocculent at the bottom. The precipitate was then collected by centrifugation at 8000 g for 5 min and washed twice with distilled water. The solid residue was dissolved in 100.0 mL of distilled water and adjusted to clarity with 1.0 N NaOH (pH=8–9). After 2 days of dialysis by deionized water (3500 Da), protein was removed by the Sevage method, and the residue was lyophilized to obtain crude polysaccharide. The EPS were purified with DEAE-52 cellulose column and dextran G-200 column.<sup>18</sup> Each component was collected by linear elution of 0–1.0 M NaCl solution using an automatic collector and was determined by the phenol-sulfuric acid method combined with ultraviolet spectrophotometry (490 nm). The main components were dialyzed with distilled water for 48 h and then lyophilized to obtain pure EPS.

## Physicochemical Properties of EPS

### Molecular Weight

Weight-average molecular weight (Mw), number-average molecular weight (Mn) and polydispersity index (Mw/Mn) of EPS were measured by gel permeation chromatography (GPC).<sup>19</sup> Twenty mg of EPS was dissolved in 10.0 mL of distilled water and filtered through a microporous membrane (0.22  $\mu\text{m}$ ). The chromatographic conditions were as follows: injection volume, 30.0  $\mu\text{L}$ ; column, Ultrahydrogel<sup>TM</sup> Linear (300 mm  $\times$  7.8 mm id  $\times$  2); flow rate, 0.5 mL/min; and temperature, 40°C. EPS samples were analyzed in an aqueous solvent system during detection.

## Monosaccharide Composition

Monosaccharide composition was detected by HPLC (Waters 1525).<sup>18</sup> Briefly, EPS was hydrolyzed in H<sub>2</sub>SO<sub>4</sub> (12 M) at 100°C under closed stirring for 2.5 h, and the obtained hydrolysate was filtered and centrifuged at 4000 g for 10 min, with the pH adjusted to 6.0 by BaCO<sub>3</sub>. The supernatant was diluted 20-fold and detected by high-performance anion-exchange chromatography with pulsed amperometric detection in a Dionex system: column, Thermo ODS-2 C18 (4.6  $\times$  250 mm, 5  $\mu\text{m}$ ); mobile phase, 0.1 mol/L phosphate buffer: acetonitrile = 82:18 (v/v), pH = 7.0; flow rate, 1.0 mL/min; temperature, 25°C; injection volume, 10.0  $\mu\text{L}$ ; and wavelength, 254 nm. Glucose, glucuronic acid, galactose, galacturonic acid, rhamnose, mannose, fructose, arabinose and fucose (Sigma, >99%) were selected for comparison.

## Observation of EPS Microstructure by Scanning Electron Microscopy (SEM)

EPS was dissolved in distilled water (20.0 mg/mL), of which 0.5 mL was freeze-dried evenly on a glass slide (2.0  $\times$  2.0 cm). The sample was coated with gold to observe the microstructure of EPS using SEM (JSM-840, JEOL, Japan).<sup>18</sup>

## Formation and Characterization of EPS Nanoparticles

EPS nanoparticles were prepared by adjusting the pH of the EPS water solution. Briefly, EPS solution (0.75%, w/v) was divided into six groups, and 1.0 M HCl was added dropwise using a microinjector under magnetic stirring. The pH was adjusted to 8, 7, 6, 5, 4 and 3, and the particle size and distribution of each group were determined by a laser scattering instrument (Zetasizer Nano ZS90, Malvern) to analyze the formation of nanoparticles under different pH conditions. In addition, each sample was processed by ultrasound (20K Scientz<sup>®</sup>) for 5 min as a control group (the average value was obtained after measurements were performed in triplicate). Next, 100.0  $\mu\text{L}$  of EPS nanoparticle solution was uniformly freeze-dried on the slide. The microstructures of the nanoparticles were observed by SEM and transmission electron microscopy (TEM, HITACHI, HT7700, Japan). SEM was performed according to the above section. Following the Song et al (2020)<sup>10</sup> method, nanoparticle-loaded copper grid was negatively stained with 2.0% phosphotungstic acid for 30 min for observation after drying. Particle size and zeta potential of nanoparticles at different pH were

determined (Zetasizer Nano ZS90, Malvern, UK) to determine the isoelectric point.<sup>20</sup>

## Emulsifying Activity of EPS at Different pH and Concentration

Emulsifying ability (emulsification index, E24, equation 1) of EPS to sunflower oil at different concentrations (0, 0.25, 0.5, 0.75, 1.0 and 1.25%) and pH (7, 6, 5, 4 and 3) was tested. After the obtained emulsions were stained with Nile red, the morphology of the emulsion droplets (eye-piece 10×, objective 100×) was observed at a 488-nm wavelength excitation light using a positive fluorescence microscope (Leica DM4B, Germany).<sup>18</sup>

$$E24 = \frac{h_e}{h_t} \times 100 \quad (1)$$

where “ $h_e$ ” is the height of the emulsion layer and “ $h_t$ ” is the overall height of the system.

## Preparation and Optimization of ECPN

### Preparation of NEs by Ultrasound

At room temperature, 0.25 mg of CT was dissolved in 3.0 mL of sunflower oil as the oil phase. Next, 0.1 g of EPS and the prescribed amount of emulsifier were dissolved in 10 mL of distilled water as the aqueous phase. Primary emulsions were obtained by adding 2.0 mL of the water phase into the ep tube, dropping 3.0 mL of the oil phase into the water phase and vortexing for 5 min (final concentration of CT was 0.005%, w/w). The NEs were then prepared by ultrasound: probe, 14 mm; amplitude, 20% (750 W); and interval, 5 s. The entire process was carried out in an ice bath for 5 min, and the temperature difference of the system did not exceed 20°C. NE droplet size was measured every 5 min.

### Optimization by the Response Surface

The set of response surface experiments was designed using Design-expert 8.0 software. Given the pH of psoriatic skin (ca. 5.8) and the need to reduce the emulsifier dosage, an EPS concentration of 1.0% and pH=6 were determined to be optimal and used in subsequent experiments. Ultrasound time ( $X_1$ ), amplitude ( $X_2$ ), PEG400 amount ( $X_3$ ) and sunflower oil amount ( $X_4$ ) were the independent variables, with high, medium and low levels for each factor (Table S1). Because the concentration of CT was low (only 0.005%) with little effect on particle size, it was not considered an independent variable. Droplet size was set as the experimental response value to optimize the minimum size. A total of 29 groups of experiments (Table S2) with 4 factors and 3 levels were

designed using the Box-Behnken Design (BBD) method; experiments were conducted in triplicate to obtain mean values. Experiments were conducted in a random order to minimize the unexplained variation stemming from external factors.<sup>21</sup>

### Characterization of the Physicochemical Properties of ECPN

ECPN types were identified by the wetting filter paper test. Briefly, 50  $\mu$ L of ECPN was dropped in the center of the filter paper; rapid spread indicated the O/W type, while a lack of spread indicated the W/O type. The dynamic viscosity of NE was measured by an electronic viscometer.<sup>22</sup> Droplet size, distribution and zeta potential were determined as described in Section “Observation of EPS microstructure by scanning electron microscopy (SEM)”.<sup>10</sup> The micromorphology of ECPN was observed by TEM as described in Section “Formation and characterization of EPS nanoparticles”.

### Stability of ECPN

The stability of ECPN was tested in triplicate (5.0 mL for each), and ECPN were placed at 25°C for 2 months. Emulsion size was measured every 6 days. After diluting 20  $\mu$ L of sample by 100 times, changes in the size at different pH (3, 4, 5, 6 and 7) were detected to study pH sensitivity and observe aggregation or separation.<sup>12</sup>

### Encapsulation Efficiency (EE)

Because of the low content of CT, detection of the content of CT in ECPN is most accurate by HPLC.<sup>23</sup> Briefly, 1.0 mL of ECPN was dissolved with methanol in a brown bottle, vortexed at 40°C, shaken, added with an appropriate amount of methanol and centrifuged at 10,000 rpm for 10 min. A small amount of the precipitate was filtered through a 0.45- $\mu$ m microporous membrane. After diluting 10.0  $\mu$ L of filtrate with 20.0  $\mu$ L ethyl acetate and 1.0 mL methanol, the CT content was detected by HPLC (100  $\mu$ L) and substituted into equation (2):

$$EE(\%) = \frac{\text{Weight of loaded CT}}{\text{Weight of initial CT}} \times 100 \quad (2)$$

### In vitro Release

Dialysis bags (3500 Da) under sink conditions loaded with 3.0 mL of ECPN were immersed in 60 mL of medium (phosphate buffer (pH=5.8) and methanol (7:3)) at 37°C in a water bath and shaking at 50 rpm. Next, 2.0 mL of the medium at 1, 2, 4, 8, 12, 24 and 36 h was collected and

replaced with an equal amount of fresh medium. After filtration with a microporous membrane (0.22  $\mu\text{m}$ ), the CT content was detected by HPLC as described in Section 2.10. The cumulative drug release was then calculated.<sup>24</sup>

## Animal Experiment and Histological Analysis of Psoriasis

All animal treatments and laboratory procedures were conducted according to the National Institutes of Health Guide for the Care and Use of Laboratory Animals (NIH Publications No. 8023, revised 1978), and approved by the Ethics Committee of Weifang Medical University (2018-103). A psoriasis mouse model was induced with imiquimod cream. Approximately 0.2 g of imiquimod cream was applied on the ears of mice (200  $\pm$  10 g) once in the morning and once in the evening for 10 days. The mice were divided into the ECPN group, positive control group, healthy group and model group. After successful modeling, medication was administered for 9 consecutive days (three times a day). During medication, surface morphology, scales thickness, erythema and erythema in the experimental areas in each group were observed by the naked eye. Area and severity of psoriasis-like lesions (erythema, scales, plaques and degree of hypertrophy) were scored by the psoriasis area and severity index (PASI) in five grades (4 points - extremely severe, 3 points - severe, 2 points - moderate, 1 point - mild and 0 points - none) (averages of 6 in each group). Mice in each group were sacrificed 24 h after the final application of cream, and ear tissues were fixed in 10% formaldehyde solution. Paraffin-embedded sections (ca. 0.5 mm of thickness) were stained with a hematoxylin and eosin (H&E) kit (Solarbio, Beijing, China).

## Data Analysis

Data were expressed as mean  $\pm$  SD and analyzed by t-tests using Origin 9.0 software.

## Results

### Strain Identification

The FYS strain produces milky white colonies with irregular edges and folded concave shapes or bulges in the middle (Figure 1A). After comparison of 16S rDNA sequences (Genbank number: MN865176), the phylogenetic tree was constructed (Figure 1B). The FYS strain clustered with *B. halotolerans* DSM 8802 NR, which had the highest homology and lowest evolutionary distance. Therefore, the strain represented a type of *B. halotolerans*.

## Preparation and Characterization of the Physicochemical Properties of EPS

The obtained EPS consisted of milky white floccules (Figure 2A). The three-dimensional network structure (Figure 2B) consisting of pinnate (Figure 2C) or irregular particles was observed by SEM. Molecular weight and monosaccharide composition data are shown in Figure 2D, Figure 2E and F and Table 1.

## Relationship Between the Formation of EPS Nanoparticles and pH

EPS solution was colorless and transparent at pH = 7–8 (Figure 3A) without nanoparticle formation in the system as indicated by observations of particle size (Figure 3B). When the pH decreased from 6 to 4, the appearance of the solution changed from colorless transparent to a clear liquid with blue fluorescence. At this time, observations of particle size indicated that nanoparticles had been generated, and the particle size increased continuously as the pH decreased (particle size ranged from 48.1 to 95.0 nm) (Figure 3B). Meanwhile, SEM (Figure 3C) and TEM (Figure 3D) images revealed the micromorphology of EPS nanoparticles. However, when pH < 3, EPS aggregates or flocculates formed large particles (particle sizes ca. 2310.8 nm), and the system became turbid. The point where the plot passed through a zeta potential of zero is called the isoelectric point. The isoelectric point was approximately 3.7 (Figure 3E). In addition, when the pH decreased from 8 to 4, the effect of ultrasound on particle size was not significant (Figure 3B). In conclusion, the above results indicate that EPS can form nanoparticles at pH 6, 5 and 4.

## Emulsifying Activity of EPS at Different pH and Concentrations

Table 2 and Figure 4A and B show that when the pH of EPS was between 4 and 6 and the concentration was between 0.5% and 1.0%, the emulsification index  $E_{24}$  remained above 70% (\*  $p < 0.05$ ). Moreover, at pH = 5 and 6, the droplet size of the emulsions was smaller. Nile red staining (Figure 4C) and size distribution results (Figure 4D) showed that when the EPS concentration was 0.75% and the pH was 6, the size distribution of the droplets was relatively narrow, with an average size of 13.1  $\mu\text{m}$ . The  $E_{24}$  was decreased when the pH of EPS was 7 or 3, and the concentration was less than 0.25%. As illustrated in Figure 3A and Figure 4A, the pH range of EPS with the strongest

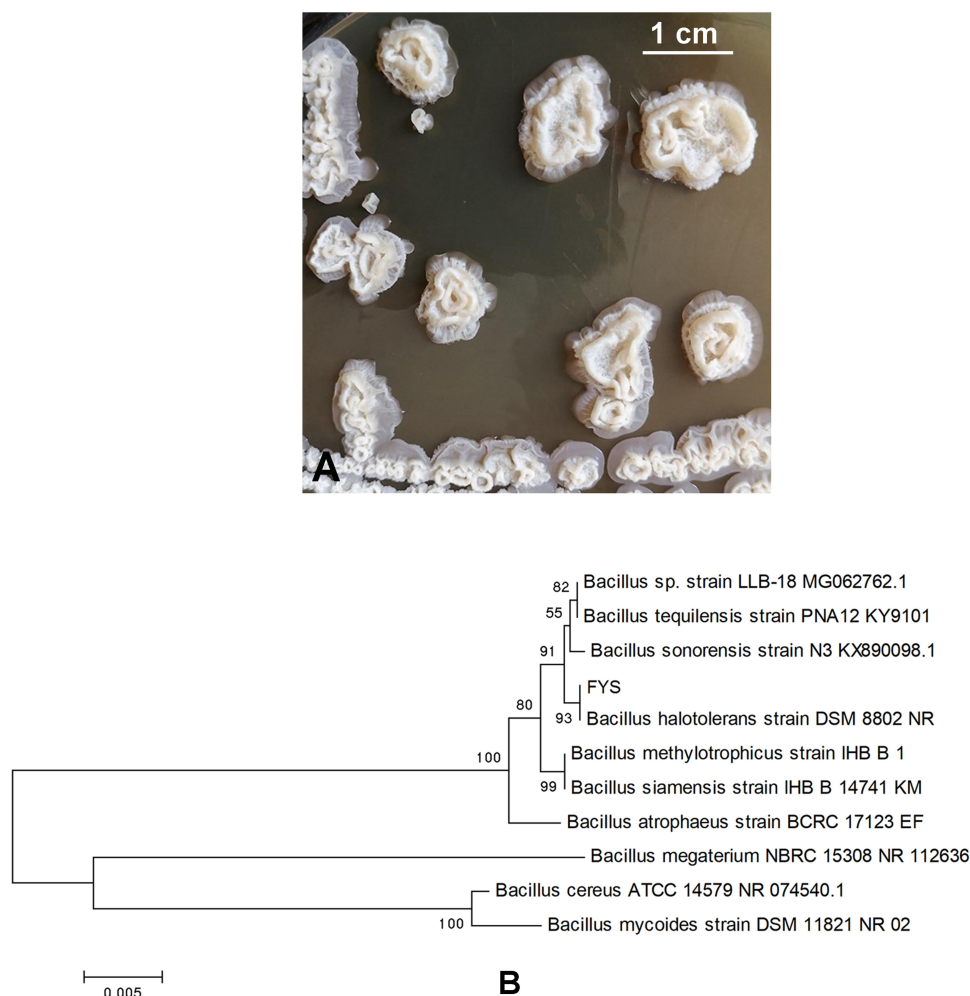


**Figure 1** (A) Colony morphology of FYS; (B) phylogenetic tree.

emulsifying activity coincided with the formation of EPS nanoparticles. In conclusion, pH has an effect on the emulsifying ability of EPS, and higher concentrations of EPS nanoparticles result in a stronger emulsifying ability.

## Preparation and Response Surface Optimization of ECPN

ECPN were prepared by ultrasound. The formulation and preparation of ECPN were optimized in combination with the BBD of the response surface (Table S2). Regression analysis was performed to obtain a quadratic multiple regression equation model (Equation 3):

$$Y = 257.00 - 11.08X_1 - 127.58X_2 - 6.83X_3 + 51.83X_4 - 26.25X_1X_2 + 7.25X_1X_3 - 4.75X_1X_4 - 0.75X_2X_3 - 50.75X_2X_4 - 19.00X_3X_4 + 8.42X_1^2 + 86.67X_2^2 + 13.79X_3^2 - 9.46X_4^2$$

(Y is the average particle size) (3)

There were significant differences between different processes of the model, and differences in the missing items were not significant ( $p > 0.05$ ), indicating that residual errors were caused by random errors (Table S3). Fitness  $R^2 > 90\%$  suggested that the model can reflect the change in the response value with high fitness.

An analysis of variance of the regression coefficient of the fitted quadratic equation revealed that  $X_2$  and  $X_4$  significantly differed in their linear effect ( $p < 0.01$ ); the rest of the differences were not significant (Table S4). Among interaction effects,  $X_2X_4$  and  $X_2^2$  had extremely significant differences ( $p < 0.01$ );  $X_1X_2$  significantly differed ( $p < 0.05$ ); and the rest were not significant. The main effect relationship of each factor was ultrasound amplitude  $>$  sunflower oil amount  $>$  ultrasound time  $>$  PEG400 amount.

Finally, the response surface was plotted using Design-expert 8.0. Figure 5A intuitively shows the effect of the

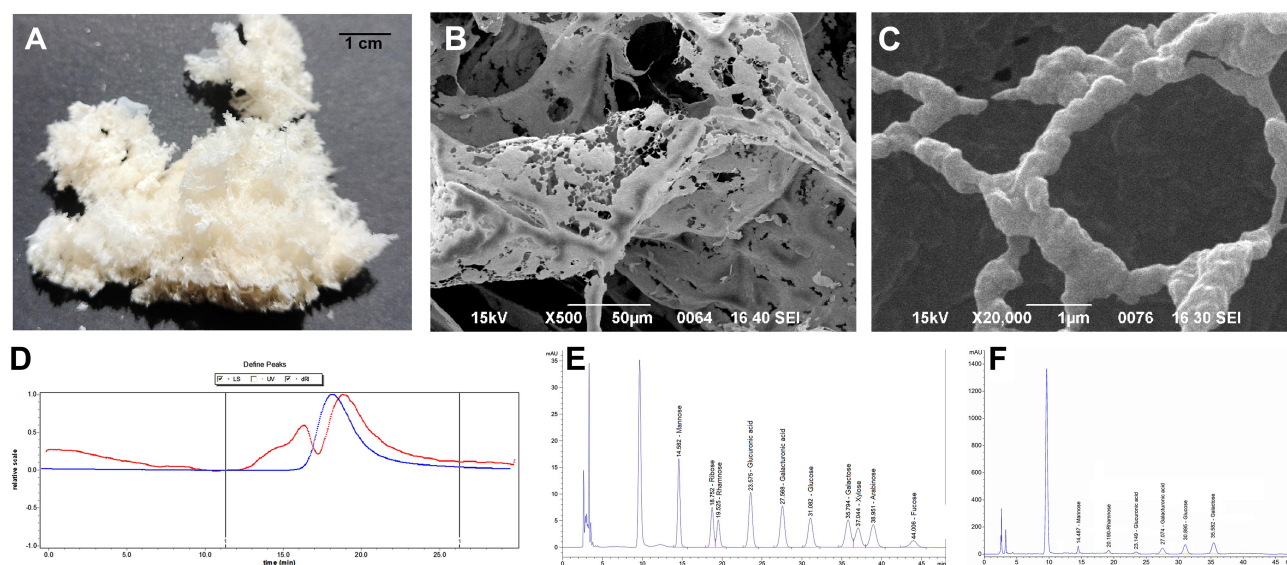


**Figure 2** (A) Lyophilized products of EPS; (B) microstructure by SEM (500 $\times$ ); and (C) microstructure by SEM (20,000 $\times$ ). (D) GPC; (E) standard curve of monosaccharide reference standard; and (F) EPS monosaccharide composition curve.

two-factor interaction on the size of emulsion droplets. As shown in Figure 5A, D and E, the slope of the response surface is steeper, which indicates that the interaction of ultrasound time and amplitude, PEG400 and amplitude, as well as sunflower oil and amplitude had a greater impact on the particle size of emulsion droplets. As the ultrasound time extended within a certain range, the amplitude increased, and the size of emulsion decreased (Figure 5A). As the amount of PEG400 and the ultrasound amplitude increased, the size of the emulsion also significantly decreased (Figure 5D). As the oil amount decreased and the amplitude increased, the emulsion size significantly decreased (Figure 5E). As illustrated in Figure 5B, C and F, the gradient of the response surface was gentle, indicating that the interaction had little effect on the emulsion size, and the response value can withstand a wide range of conditions.

The optimized process parameters and validation results (Table S5) were obtained through the above regression model. When the EPS concentration was 1.0%, pH 6, ultrasound time ( $X_1$ ) 5.75 min, power ( $X_2$ ) 24.71%, co-emulsifier ( $X_3$ ) 2.48% and the oil ratio ( $X_4$ ) 1.02%, the prepared NE had a particle size of only 170.8 nm.

## Physicochemical Properties and Stability of ECPN

After detection, ECPN were O/W-type (Figure 6A) with a dynamic viscosity of approximately  $101.8 \pm 8.5$  mPa·s. The Dyndallphenomenon (Figure 6B) was observed. Droplet size and zeta potential were 170.8 nm (Figure 6C) and  $-30.1$  mV (Figure 6D), respectively. TEM showed that the ECPN were spherical (Figure 6E). The emulsion droplets were in the form of small particles, and EPS nanoparticles could be clearly observed adsorbing on the surface of the oil droplets (Figure 6F) under high magnification. The microstructure of ECPN under TEM was consistent with the Pickering emulsification mechanism described above. The size of emulsion droplets was in the range of 170.8–287.0 nm at pH = 5–6 for 2 months at 25°C without phase separation (Figure 6G), indicating high static stability. At pH = 4 or 7, the size increased (195.0–893.1 nm); the size increased especially sharply at pH = 3 (Figure 6H).

## EE and in vitro Release

The EE of ECPN was approximately 89.2%. The cumulative release of ECPN reached  $95.0 \pm 4.0\%$  at 36 h, and that

**Table I** Molecular Weights and Monosaccharide Ratio of EPS

Sample	Molecular Weight			Monosaccharide Ratio (%)					
	Mn/Da	Mw/Da	Mw/Mn	Glucose	Galactose	Glucuronic acid	Rhamnose	Galacturonic Acid	Mannose
EPS	$3.478 \times 10^3$	$4.362 \times 10^3$	1.254	32.0	34.3	9.7	7.4	10.3	6.3

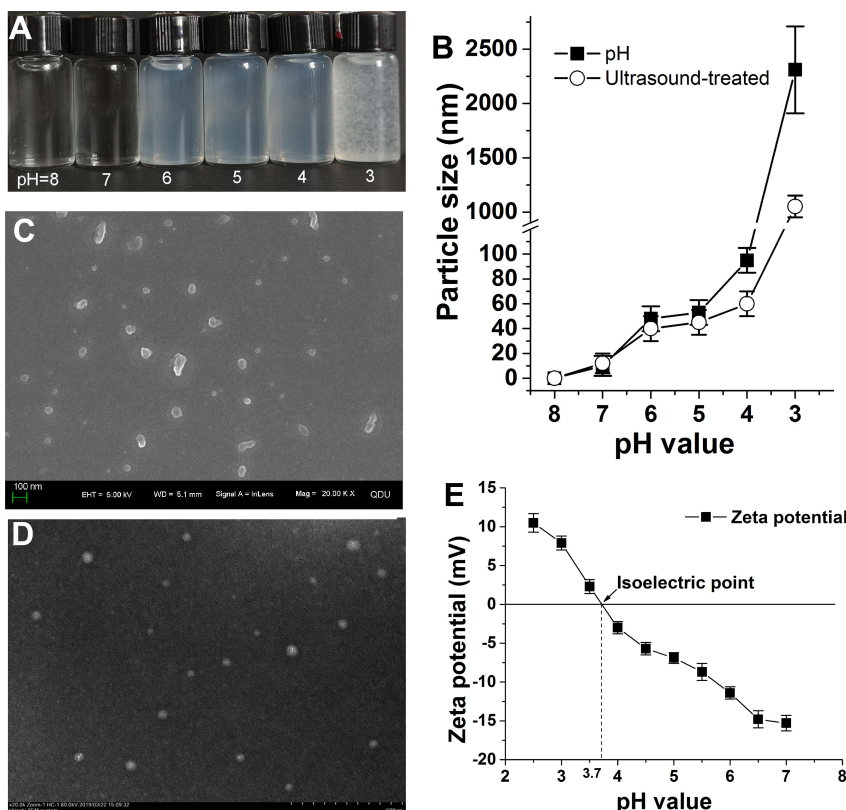


**Figure 3** (A) Formation of nanoparticles when EPS changes with pH; (B) change in average particle size of EPS nanoparticles; (C) micromorphology of EPS nanoparticles by SEM (pH=6); (D) micromorphology of EPS nanoparticles by TEM (pH=6); (E) isoelectric point.

of free CT was  $93.1 \pm 6.0\%$  at 12 h (Figure 7). The release time of ECPN was approximately three times longer than that of free CT, reflecting a sustained-release effect.

### PASI Score and HE Staining

Imiquimod-induced psoriasis models in mice are currently one of the most widely used methods. In the normal group, the ear cuticle was thin and intact with complete keratinization and no inflammatory cell infiltration (Figure 8A). On the 9th day of modeling, the epidermis of the model group showed psoriasis-

like symptoms, such as breakage, redness, swelling and plaque, incomplete keratinization of the epidermis, clubbing hyperplasia of the epidermis and infiltration and aggregation of a large number of lymphocytes and neutrophils (Figure 8B). The modeling process took 10 days; medication was then applied, and the PASI score was performed (Table 3). On the 3rd day of medication, inflammation and keratosis in the ECPN group was significantly alleviated and was close to the effect of the positive control group. On the 6th day, redness, scales and plaques disappeared, and some hair recovered

**Table 2** E<sub>24</sub> of EPS at Different pH and Concentrations (\* p < 0.05)

EPS Concentration	E <sub>24</sub>				
	pH=7	pH=6	pH=5	pH=4	pH=3
1.0%	65.1 ± 1.3	72.5* ± 0.7	72.1* ± 1.1	70.5* ± 1.0	12.5 ± 2.0
0.75%	53.3 ± 1.0	72.5* ± 0.6	72.0* ± 1.2	70.4* ± 1.1	5.8 ± 1.9
0.5%	50.7 ± 1.3	64.9 ± 1.0	50.6 ± 1.5	47.2 ± 1.7	0
0.25%	31.0 ± 0.9	28.2 ± 0.8	25.2 ± 1.8	26.7 ± 2.3	0
0.125%	9.9 ± 1.6	17.4 ± 2.9	17.1 ± 2.3	16.2 ± 3.1	0
0	0	0	0	0	0

**Notes:** Mean values (±standard deviation) within the same column that did not share a common superscript indicate a significant difference (\* P < 0.05).



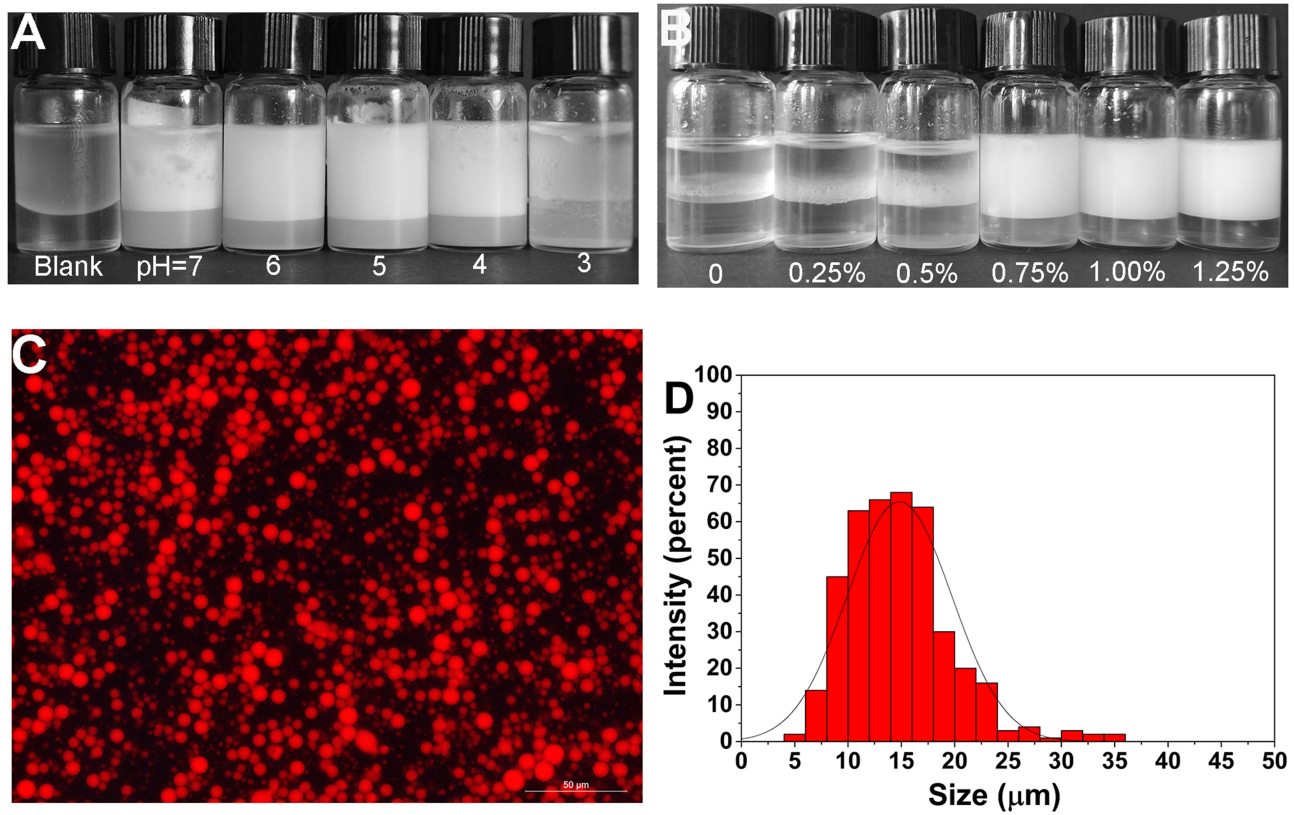


**Figure 4** (A) The emulsifying activity of EPS at different pH (concentration is 0.75%); (B) emulsifying behavior of EPS at different concentrations (pH=6); (C and D) Nile red staining to observe the shape and size distribution of emulsions (concentration is 0.75%, pH=6).

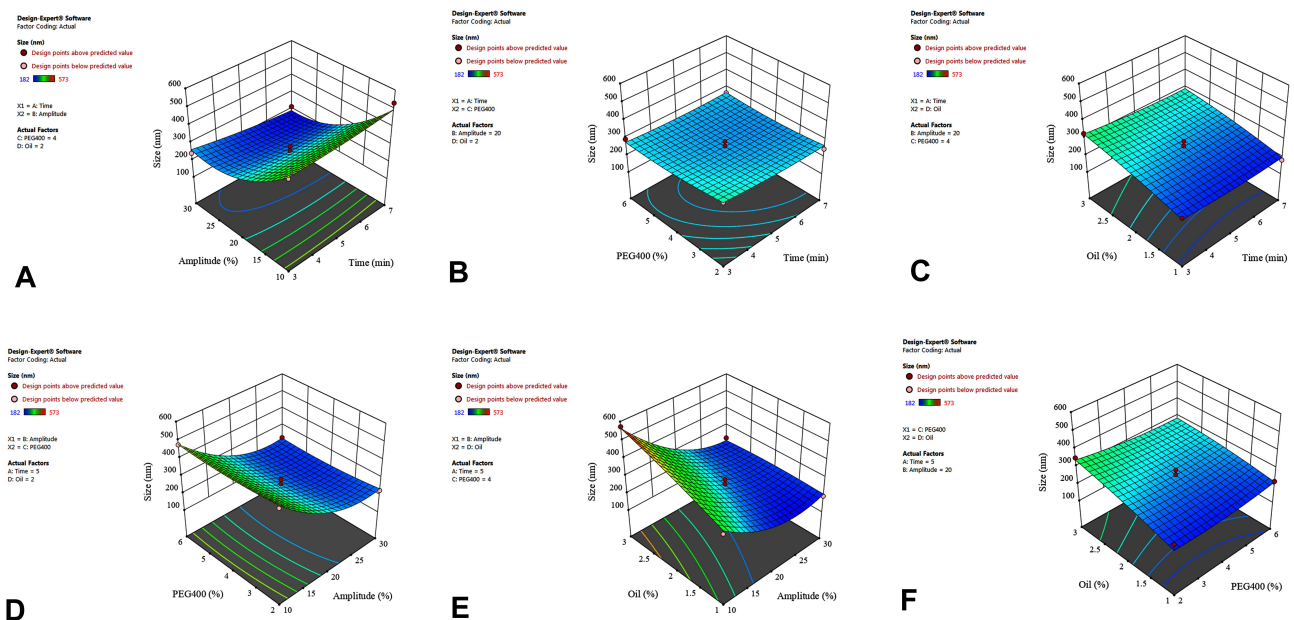


**Figure 5** Response surface plot showing the significant ( $p < 0.05$ ) interaction effect for droplet size as a function of (A) ultrasonic amplitude and ultrasonic time; (B) ultrasonic time and PEG400 content; (C) ultrasonic time and oil content; (D) PEG400 content and ultrasonic amplitude; (E) oil content and ultrasonic amplitude; and (F) PEG400 content and oil content.

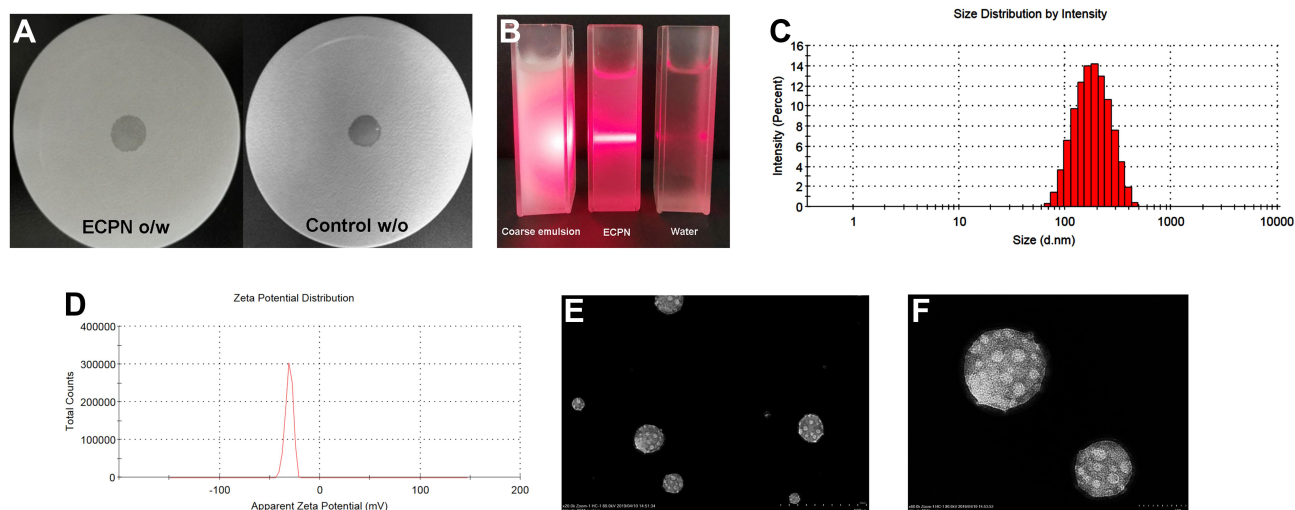


**Figure 6** (A) NE type; (B) Tyndall effect; (C) droplet size distribution; (D) zeta potential; (E/F) morphology of ECPN at pH=6 by TEM (500 nm  $\times$ ; 100 nm  $\times$ ); (G) droplet size changes of ECPN stored at pH=6; and (H) storage stability of ECPN at different pH.

in the ECPN group (Figure 8C); this process in the ECPN group was shorter than that of the positive control group (9 days) (\*  $p < 0.05$ ).

## Discussion

The remarkable emulsifying activity of EPS indicates that they have much potential to be used as emulsifiers. The emulsification mechanism includes the following: 1) formation of an extended network in the continuous phase;<sup>25</sup> and 2) formation of an emulsified film on the surface of emulsion droplets.<sup>10</sup> We found that the emulsifying ability of EPS produced by *B. halodurans* FYS strain varied with

pH and was stronger in the form of nanoparticles. EPS nanoparticles adhere to the surface of oil droplets as solid particles to stabilize the emulsions via a Pickering emulsification mechanism.

The *B. halodurans* FYS strain was screened from the marine mangrove system. The bacteria are primarily used in papermaking, enzyme production, wastewater treatment and environmental manipulation.<sup>26</sup> Here, we study the EPS produced by this strain and its Pickering emulsification mechanism for the first time.

The molecular weight of EPS varies from tens of thousands to millions. Most of the EPS produced by *Bacillus sp.* are heteropolysaccharide macromolecules composed of two or more monosaccharides with extremely complex structures. For example, EPS produced by *B. licheniformis* PASS26 consist of glucose, galactose, fructose, mannose and galacturonic acid.<sup>27</sup> The EPS exhibit a three-dimensional pinnate network structure under SEM and are composed of irregular particles. Most studies consider EPS to have a highly branched porous network structure.<sup>28</sup> For example, two types of EPS produced by *B. amyloliquefaciens* LPL061 have three-dimensional network structures and are composed of hexagonal and irregular particles.<sup>29</sup> EPS with this structure tend to have higher viscosity or thickening capacity, which is beneficial for stabilizing emulsions.<sup>18,30</sup> These properties provide a structural basis for the preparation of stable emulsions or NE by EPS.

The EPS can be prepared into nanoparticles by adjusting the pH. When the pH was 7, the EPS solution was colorless and transparent, possibly because acidic groups (such as carboxyl groups) in the EPS structure were

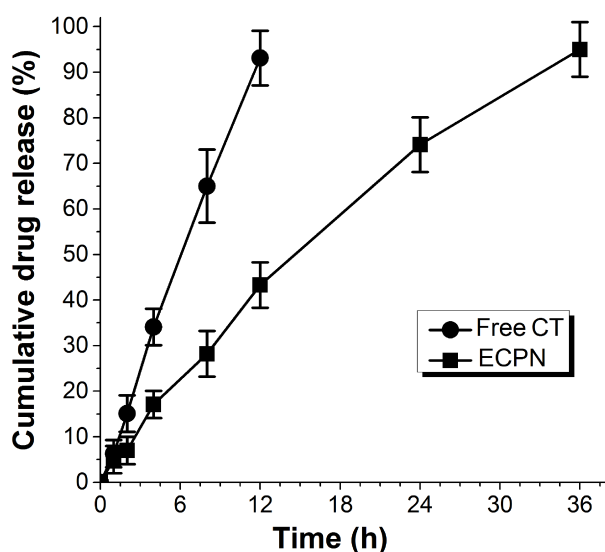


**Figure 7** In vitro drug release profiles of ECPN.

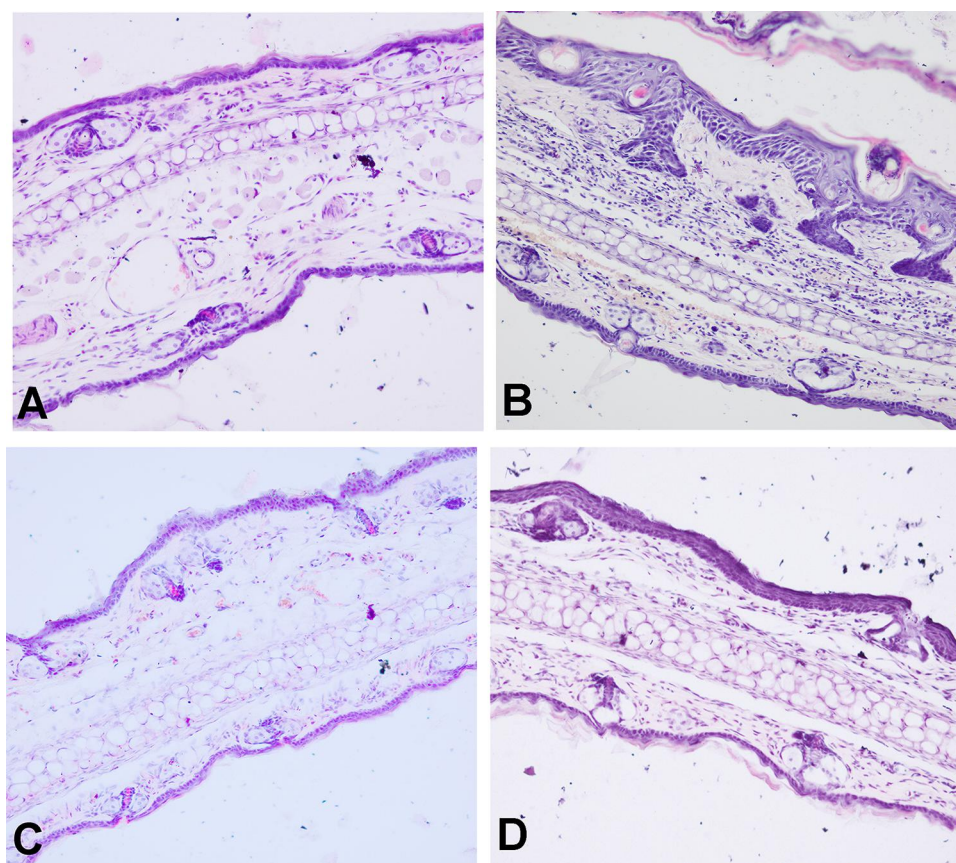


**Figure 8** HE staining. (A) Healthy group (200 ×); (B) model group; (C) ECPN group; and (D) positive control group.

destroyed under alkaline conditions, resulting in a disordered and random configuration.<sup>31</sup> As the pH decreased from 6 to 4, EPS began to form nanoparticles. On the one hand, when pH gradually approaches the isoelectric point, electrostatic repulsion between EPS molecules gradually decreases, and the interaction force between molecules gradually weakens, resulting in increased molecular collision and aggregation. On the other hand, at lower pH, the formation of intramolecular and intermolecular hydrogen bonds of EPS gradually increases, and particles aggregate.<sup>20</sup> When the pH was below the isoelectric point of EPS (ca. 3.7) or near 3, particle size increased sharply, and flocculation in the system may occur completely. EPS exists in the colloidal form when dissolved in water and is susceptible to environmental influence. When pH changes, the equilibrium in the colloidal structure is easily destroyed and reconstructed.<sup>20</sup> Dogsa (2005)<sup>32</sup> found that the structure of EPS produced by bacteria in the Northern Adriatic Sea changes at different pH. When the pH decreases from 11.0 to 0.7, the average particle size increases continuously (from 19 to 52 nm) and is attributed to the rearrangement

of the EPS structure caused by changes in pH. The formation of EPS nanoparticles depends on their composition and characteristics, and EPS produced by different microorganisms may differ.<sup>20</sup> The pH range of EPS forming nanoparticles in this study was narrow, which indicated that EPS were pH-sensitive.

Previous studies have examined the preparation of nanoparticles by EPS. For example, EPS (mannose, glucose and galactose) produced by *Lactobacillus plantarum* LCC-605 strain isolated from kimchi by Li et al (2017)<sup>33</sup> can be prepared into degradable nanoparticles for biological anti-fouling, such as the adsorption of heavy metal ions. Song (2020)<sup>10</sup> successfully prepared a NE with EPS produced by *B. vallismortis* WF4 strain using an ultrasound-assisted technique to encapsulate nystatin, which ultimately enhanced the treatment effect of candidal vaginitis and initiated the application of EPS in NE. However, no studies to date have examined EPS in Pickering emulsion.

EPS have stronger emulsifying ability in the form of nanoparticles (pH = 4–6). Their stronger emulsifying ability is likely explained by the fact that EPS nanoparticles play an important role in the emulsification process; in addition,

**Table 3** PASI Score

Groups	Medication Days								
	1	2	3	4	5	6	7	8	9
Healthy	0.00	0.00	0.00	0.00	0.00	0.00	0.00	0.00	0.00
Model	4.00	4.00	4.00	3.83	3.60	3.60	3.30	3.10	2.93
ECPN	3.30	3.10	2.73	2.17	1.80	1.37	1.07	0.90	0.93
Positive control	3.43	3.13	2.93	2.83	2.37	1.93	1.57	1.40	1.07

smaller particle sizes and larger concentrations also result in stronger emulsifying activity. Changes in pH result in changes in the particle size of EPS; thus, pH is an important factor affecting the stability of emulsions. Nanoparticles can be used as emulsifiers for the stabilization of Pickering emulsions. Qi et al (2014)<sup>34</sup> found that smaller poly (D, L-lactic-co-glycolic acid) (PLGA) nanoparticles (with a particle size of 300 nm) can be adsorbed on the surface of oil droplets, form a dense layer to prevent emulsion droplet aggregation and reduce surface tension. Particles with smaller sizes are more efficient than larger ones (620.0–1150.0 nm) in terms of their emulsifying ability. Wang et al (2016)<sup>35</sup> prepared five types of nanocellulose crystals with different particle sizes (178.2–261.8 nm) by adjusting the acid hydrolysis time of cellulose and used them to emulsify palm oil to produce Pickering emulsions. The results showed that smaller cellulose crystal particles corresponded to higher emulsification efficiency.

Both pH and concentration have an effect on the emulsifying ability of EPS, and the emulsifying ability of EPS nanoparticles increases with concentration in a concentration-dependent manner. Solid particles form a protective layer during adsorption on the oil–water interface to stabilize the emulsions. As the particle concentration increases, the solid particles on the oil–water interface increase and the protective layer becomes denser. In addition, redundant particles also enter the continuous phase and distribute between the emulsion droplets, hindering the collision and aggregation of droplets and thereby stabilizing the system.<sup>36,37</sup> This observation is consistent with the results of our study and may explain the concentration-dependent pattern.

The above results indicate that pH may affect the emulsifying ability of EPS by influencing the spatial configuration and flocculation of EPS to form nanoparticles and changing particle size. In conclusion, EPS show much potential to be used as a Pickering emulsifier.

Pickering emulsions are known to have better stability. The solid film formed by nanoparticles on the surface of

oil droplets hinders the flow, deformation and aggregation of emulsion droplets. Removing the adsorbed particles from the interface requires high energy.<sup>38</sup> Thus, the stability of Pickering emulsion is primarily affected by factors, such as pH and ionic strength, but is less affected by gravity and mechanical force.<sup>39</sup> For example, Kalashnikova et al (2011)<sup>40</sup> emulsified hexadecane with the hydrolysates of bacterial cellulose to prepare stable O/W-type Pickering emulsions. Highly stable NE prepared with cellulose nanocrystals and cellulose nanofibrils can remain unchanged for months.<sup>13</sup> Moreover, Pickering emulsions have superior stability compared with emulsions formed by surfactant emulsifiers.<sup>41</sup>

One of the reasons for the sustained release effect of ECPN is the viscosity, which makes the drug disperse uniformly and diffuse slowly into the medium.<sup>10</sup> Second, the micro-gap between the adsorbed nanoparticles on the surface of ECPN droplets slows drug release, avoiding the burst release and reducing drug toxicity.<sup>42</sup> Clobetasol propionate and CT nanoemulsion prepared by Kaur et al (2017)<sup>24</sup> can completely release CT at 10 h.

The pH of ECPN is close to that of the internal environment of psoriasis skin, which is conducive to the stability of ECPN and ensures the slow release of the drug. Multiple immune cells (such as neutrophils, dendritic cells and CD4<sup>+</sup> T cells) are activated in psoriasis and interact with KC to promote KC proliferation and differentiation.<sup>43</sup> H&E staining showed that the number of these immune cells was decreased when ECPN alleviated inflammation in psoriasis. For example, methotrexate topical NE, which was first reported in 2014, can effectively inhibit KC proliferation and the inflammatory response.<sup>44</sup> In conclusion, the animal experiments revealed that the ECPN have a superior therapeutic effect and effectively shorten the treatment course of psoriasis. The efficacy of ECPN may depend on the large dispersion and specific surface area of ECPN themselves, as well as the sustained-release effect, which can make the drug disperse more uniformly with longer action time and

accumulate in greater concentrations on the skin.<sup>24</sup> In addition, EPS are natural polysaccharides that have several advantageous properties, including antioxidant capacity, high water absorption and moisturizing properties, as well as biocompatibility, bioadhesion and biodegradability.

## Conclusion

EPS produced by the marine bacterium *B. Halodurans* FYS strain can form nanoparticles in the pH range of 4–6 and has stronger emulsifying activity and stability in the form of nanoparticles because of the Pickering emulsification mechanism of EPS nanoparticles. Stable and sustained-release Pickering NE, ECPN, were prepared by ultrasound and response surface optimization, which effectively shortened the treatment course of psoriatic mice. This study broadens the range of its application as emulsifiers, provides new insight into the mechanism of EPS in Pickering emulsification and contributes new ideas for the treatment of psoriasis vulgaris.

## Acknowledgments

This work was supported by National Science Foundation of China (No. 81903568 and No. 31570941).

## Disclosure

The authors report no conflicts of interest in this work.

## References

- Satpute SK, Banat IM, Dhakephalkar PK, et al. Biosurfactants, bioemulsifiers and exopolysaccharides from marine microorganisms. *Biotechnol Adv.* 2010;28(4):436–450. doi:10.1016/j.biotechadv.2010.02.006
- Carrión O, Delgado L, Mercade E. New emulsifying and cryoprotective exopolysaccharide from Antarctic *Pseudomonas* sp. ID1. *Carbohydr Polym.* 2015;117:1028–1034. doi:10.1016/j.carbpol.2014.08.060
- Song B, Zhu W, Song R, et al. Exopolysaccharide from *Bacillus vallismortis* WF4 as an emulsifier for antifungal and antipruritic peppermint oil emulsion. *Int J Biol Macromol.* 2019;125:436–444. doi:10.1016/j.ijbiomac.2018.12.080
- Margaret PH. Under their skin. *Nature.* 2012;492:64–65. doi:10.1038/492S64a
- Pradhan M, Singh D, Singh MR. Novel colloidal carriers for psoriasis: current issues, mechanistic insight and novel delivery approaches. *J Control Release.* 2013;170(3):380–395. doi:10.1016/j.jconrel.2013.05.020
- Kaushik SB, Lebowitz MG. Psoriasis: which therapy for which patient: focus on special populations and chronic infections. *J Am Acad Dermatol.* 2019;80(1):43–53. doi:10.1016/j.jaad.2018.06.056
- Crawshaw AA, Griffiths CEM, Young HS. Investigational VEGF antagonists for psoriasis. *Expert Opin Investig Drugs.* 2012;21(1):33–43. doi:10.1517/13543784.2012.636351
- Frieder J, Kivelevitch D, Menter A. Calcipotriene betamethasone dipropionate aerosol foam in the treatment of plaque psoriasis: a review of the literature. *Ther Deliv.* 2017;8(9):737–746. doi:10.4155/tde-2017-0058
- Rai VK, Mishra N, Yadav KS, et al. Nanoemulsion as pharmaceutical carrier for dermal and transdermal drug delivery: formulation development, stability issues, basic considerations and applications. *J Control Release.* 2018;270(December2017):203–225. doi:10.1016/j.jconrel.2017.11.049
- Song R, Yan F, Cheng M, et al. Ultrasound-assisted preparation of exopolysaccharide/nystatin nanoemulsion for treatment of vulvovaginal candidiasis. *Int J Nanomedicine.* 2020;15:2027–2044. doi:10.2147/IJN.S241134
- Pickering SU. Emulsions. *J Chem Soc.* 1907;91:2001–2021. doi:10.1039/CT9079102001
- Mady SP, Nicolas A, Ysia IG, et al. Pickering nano-emulsion as a nanocarrier for pH-triggered drug release. *Int J Pharm.* 2018;549(1–2):299–305. doi:10.1016/j.ijpharm.2018.07.066
- Jiménez Saelices C, Capron I. Design of Pickering Micro- and Nanoemulsions Based on the Structural Characteristics of Nanocelluloses. *Biomacromolecules.* 2018;19(2):460–469. doi:10.1021/acs.biomac.7b01564
- Sadeghpour A, Pirolt F, Glatter O. Submicrometer-sized pickering emulsions stabilized by silica nanoparticles with adsorbed oleic acid. *Langmuir.* 2013;29(20):6004–6012. doi:10.1021/la4008685
- Chevalier Y, Bolzinger MA. Emulsions stabilized with solid nanoparticles: pickering emulsions. *Coll Surf a Phys Eng Asp.* 2013;439:23–34. doi:10.1016/j.colsurfa.2013.02.054
- Sambrook J, Fritsch EF, Maniatis T. *Preparation and Analysis of Eukaryotic Genomic DNA. In Molecular Cloning: A Laboratory Manual.* 2nd ed. Beijing, China: Cold Spring Harbor Laboratory Press; 1989:367–370.
- Zhu W, Wang Y, Yan F, et al. Physical and chemical properties, percutaneous absorption-promoting effects of exopolysaccharide produced by *Bacillus atrophaeus* WYZ strain. *Carbohydr Polym.* 2018;192:(March):52–60. doi:10.1016/j.carbpol.2018.03.063
- Prasanna PHP, Bell A, Grandison AS, et al. Emulsifying, rheological and physicochemical properties of exopolysaccharide produced by *Bifidobacterium longum* subsp. *infantis* CCUG 52486 and *Bifidobacterium infantis* NCIMB 702205. *Carbohydr Polym.* 2012;90(1):533–540. doi:10.1016/j.carbpol.2012.05.075
- Xu R, Shen Q, Ding X, et al. Chemical characterization and antioxidant activity of an exopolysaccharide fraction isolated from *Bifidobacterium animalis* RH. *Eur Food Res Technol.* 2011;232(2):231–240. doi:10.1007/s00217-010-1382-8
- Wang LL, Wang LF, Ren XM, et al. PH dependence of structure and surface properties of microbial EPS. *Environ Sci Technol.* 2012;46(2):737–744. doi:10.1021/es203540w
- Anarjan N, Mirhosseini H, Baharin BS, et al. Effect of processing conditions on physicochemical properties of astaxanthin nanodispersions. *Food Chem.* 2010;123(2):477–483. doi:10.1016/j.foodchem.2010.05.036
- Sombatmankhong K, Sanchavanakit N, Pavasant P, et al. Bone scaffolds from electrospun fiber mats of poly(3-hydroxybutyrate), poly(3-hydroxybutyrate-co-3-hydroxyvalerate) and their blend. *Polymer.* 2007;48(5):1419–1427. doi:10.1016/j.polymer.2007.01.014
- Sonawane R, Harde H, Katariya M, et al. Solid lipid nanoparticles-loaded topical gel containing combination drugs: an approach to offset psoriasis. *Expert Opin Drug Deliv.* 2014;11(12):1833–1847. doi:10.1517/17425247.2014.938634
- Kaur A, Katiyar SS, Kushwah V, et al. Nanoemulsion loaded gel for topical co-delivery of clobetasol propionate and calcipotriol in psoriasis. *Nanomed Nanotech Biol Med.* 2017;13(4):1473–1482. doi:10.1016/j.nano.2017.02.009
- Bouyer E, Mekhloufi G, Rosilio V, et al. Proteins, polysaccharides, and their complexes used as stabilizers for emulsions: alternatives to synthetic surfactants in the pharmaceutical field? *Int J Pharm.* 2012;436(1–2):359–378. doi:10.1016/j.ijpharm.2012.06.052
- Kumar V, Satyanarayana T. Thermo-alkali-stable xylanase of a novel polyextremophilic *Bacillus halodurans* TSEV1 and its application in biobleaching. *Int Biodeterior Biodegrad.* 2012;75:138–145. doi:10.1016/j.ibiod.2012.09.007

27. Insulkar P, Kerkar S, Lele SS. Purification and structural-functional characterization of an exopolysaccharide from *Bacillus licheniformis* PASS26 with in-vitro antitumor and wound healing activities. *Int J Biol Macromol.* 2018;120:1441–1450. doi:10.1016/j.ijbiomac.2018.09.147
28. Yang Y, Feng F, Zhou Q, et al. Isolation, purification and characterization of exopolysaccharide produced by *Leuconostoc pseudomesenteroides* YF32 from soybean paste. *Int J Biol Macromol.* 2018;114:529–535. doi:10.1016/j.ijbiomac.2018.03.162
29. Han Y, Liu E, Liu L, et al. Rheological, emulsifying and thermo-stability properties of two exopolysaccharides produced by *Bacillus amyloliquefaciens* LPL061. *Carbohydr Polym.* 2015;115:230–237. doi:10.1016/j.carbpol.2014.08.044
30. Wang J, Zhao X, Tian Z, et al. Characterization of an exopolysaccharide produced by *Lactobacillus plantarum* YW11 isolated from Tibet Kefir. *Carbohydr Polym.* 2015;125:16–25. doi:10.1016/j.carbpol.2015.03.003
31. Zhang G, Li X, Jiang M, et al. Model system for surfactant-free emulsion copolymerization of hydrophobic and hydrophilic monomers in aqueous solution. *Langmuir.* 2000;16(24):9205–9207. doi:10.1021/la000453h
32. Dogsa I, Kriechbaum M, Stopar D, et al. Structure of bacterial extracellular polymeric substances at different pH values as determined by SAXS. *Biophys J.* 2005;89(4):2711–2720. doi:10.1529/biophysj.105.061648
33. Li C, Zhou L, Yang H, et al. Self-Assembled Exopolysaccharide Nanoparticles for Bioremediation and Green Synthesis of Noble Metal Nanoparticles. *ACS Appl Mater Interfaces.* 2017;9(27):22808–22818. doi:10.1021/acsami.7b02908
34. Qi F, Wu J, Sun G, et al. Systematic studies of Pickering emulsions stabilized by uniform-sized PLGA particles: preparation and stabilization mechanism. *J Mater Chem B.* 2014;2(43):7605–7611. doi:10.1039/C4TB01165A
35. Wang W, Du G, Li C, et al. Preparation of cellulose nanocrystals from asparagus (*Asparagus officinalis* L.) and their applications to palm oil/water Pickering emulsion. *Carbohydr Polym.* 2016;151:1–8. doi:10.1016/j.carbpol.2016.05.052
36. Abend S, Lagaly G. Bentonite and double hydroxides as emulsifying agents. *Clay Miner.* 2001;36(4):557–570. doi:10.1180/0009855013640009
37. Thieme J, Abend S, Lagaly G. Aggregation in Pickering emulsions. *Colloid Polym Sci.* 1999;277(2–3):257–260. doi:10.1007/PL00013752
38. Qin S, Yong X. Controlling the stability of Pickering emulsions by pH-responsive nanoparticles. *Soft Matter.* 2019;15(16):3291–3300. doi:10.1039/C8SM02407C
39. Li XM, Xie QT, Zhu J, et al. Chitosan hydrochloride/carboxymethyl starch complex nanogels as novel Pickering stabilizers: physical stability and rheological properties. *Food Hydrocoll.* 2019;93(December2018):215–225. doi:10.1016/j.foodhyd.2019.02.021
40. Kalashnikova I, Bizot H, Cathala B, et al. New pickering emulsions stabilized by bacterial cellulose nanocrystals. *Langmuir.* 2011;27(12):7471–7479. doi:10.1021/la200971f
41. Wu J, Ma G-H. Recent Studies of Pickering Emulsions: particles Make the Difference. *Small.* 2016;12(34):4633–4648. doi:10.1002/smll.201600877
42. Panonnummal R, Sabitha M. Anti-psoriatic and toxicity evaluation of methotrexate loaded chitin nanogel in imiquimod induced mice model. *Int J Biol Macromol.* 2018;110:245–258. doi:10.1016/j.ijbiomac.2017.10.112
43. Bonifati C, Ameglio F. Cytokines in psoriasis. *Int J Dermatology.* 1999;38(4):241–251. doi:10.1046/j.1365-4362.1999.00622.x
44. Pinto MF, Moura CC, Nunes C, et al. A new topical formulation for psoriasis: development of methotrexate-loaded nanostructured lipid carriers. *Int J Pharm.* 2014;477(1–2):519–526. doi:10.1016/j.ijpharm.2014.10.067

## International Journal of Nanomedicine

Dovepress

### Publish your work in this journal

The International Journal of Nanomedicine is an international, peer-reviewed journal focusing on the application of nanotechnology in diagnostics, therapeutics, and drug delivery systems throughout the biomedical field. This journal is indexed on PubMed Central, MedLine, CAS, SciSearch®, Current Contents®/Clinical Medicine,

Journal Citation Reports/Science Edition, EMBase, Scopus and the Elsevier Bibliographic databases. The manuscript management system is completely online and includes a very quick and fair peer-review system, which is all easy to use. Visit <http://www.dovepress.com/testimonials.php> to read real quotes from published authors.

Submit your manuscript here: <https://www.dovepress.com/international-journal-of-nanomedicine-journal>